INTERNATIONAL JOURNAL OF CLIMATOLOGY
Int. J. Climatol. **22**: 1527–1542 (2002)
Published online in Wiley InterScience (www.interscience.wiley.com). DOI: 10.1002/joc.783

LUNI-SOLAR TIDAL INFLUENCES ON CLIMATE VARIABILITY

NORMAN C. TRELOAR*
Queensland Centre for Climate Applications, Queensland Department of Primary Industries, Box 102, Toowoomba, Queensland 4350, Australia

Received 12 February 2001
Revised 21 January 2002
Accepted 23 January 2002

ABSTRACT

A possible exogenous cause of some terrestrial climate variability on time scales of 1 to 100 years is examined. Luni-solar effects, and especially the coincidences of New Moon with small perigee distance, produce important tidal perturbations. These influences have been resolved in two orthogonal directions, and the variability in the southern oscillation and sea-surface temperature anomalies may be at least partly understandable as a reflection of these tidal components. The correlation between tidal components and these climate factors is significant. The predictability of tidal effects may make a contribution to improving the accuracy and lead time of climate forecasting. Copyright © 2002 Royal Meteorological Society.

KEY WORDS: southern oscillation index (SOI); inter-decadal Pacific oscillation (IPO); luni-solar; tidal; time series analysis; equatorial; meridional

1. INTRODUCTION

The southern oscillation (SO) is an atmospheric oscillation in the surface pressure gradient over the equatorial Pacific. With the coupled changes in sea-surface temperature (SST), it is a major proximate cause of terrestrial climate variability, particularly in the tropics and mid-latitudes. The SO is conveniently measured by the monthly SO index (SOI), which incorporates the sea-level pressure difference between Papeete (Tahiti) and Darwin. R.J. Allan, P.D. Jones and others have reconstructed the variation of the monthly SOI from AD 1866 to the present (http://www.dar.csiro.au/nino/SOItable.htm). The SOI is a predictor of rainfall in the near-term (Stone and Auliciems, 1992; Stone *et al*., 1996) and has considerable economic utility, including the management of crop production (Hammer *et al*., 1996).

El Niño–SO (ENSO) effects are modulated by the inter-decadal variability of Pacific oscillations with mid-latitude or extra-tropical character (Gershunov and Barnett, 1998; Power *et al*., 1999). As an example, the inter-decadal Pacific oscillation (IPO) is an oscillation derived from global SST data, as an empirical orthogonal function (EOF) in the band-filtered three-monthly HADlsst1.1 data set updated with MOHSST6 data from the UK Meteorological Office (UKMO). The IPO data set was obtained through the courtesy of Scott Power of the Bureau of Meteorology, Melbourne. The unfiltered UKMO data set was obtained through the courtesy of Chris Folland. The IPO may be an important forecasting factor in meteorology and crop production (Power *et al*., 1999; Meinke *et al*., 2000). Another oscillation, the Pacific decadal oscillation (PDO), is derived as an EOF from SST data in the Pacific north of 20 °N (Mantua *et al*., 1997). The PDO is correlated with the IPO (Chris Folland, personal communication) and with two other Pacific SST indices and the SOI (Mantua *et al*., 1997). In North America, warm and cold PDO extremes are associated with climate

* Correspondence to: Norman C. Treloar, Queensland Centre for Climate Applications, Queensland Department of Primary Industries, Box 102, Toowoomba, Queensland 4350, Australia; e-mail: treloan@dpi.qld.gov.au

anomalies similar to those of El Niño and La Niña events (Latif and Barnett, 1996; Mantua *et al*., 1997; Zhang *et al*., 1997).

It is of interest to examine the cause of temporal variation in the SO, IPO and related climate oscillations. Astronomical influences on climate have been suggested on decadal time scales, notably from the variation in solar radiative output and from tidal effects deriving especially from the 18.6 year cycle of the Moon's nodes (e.g. Burroughs, 1992; Currie and Vines, 1996; Cerveny and Shaffer, 2001). The radiative factor will not be discussed here, and this paper will be confined to exploring tidal influences on climate variability.

On various time scales, links have been suggested between climate, astronomical tidal forces, Earth rotation, and ocean circulation and mixing. For example, changes to the Earth's rotation are driven by: (1) internal processes involving conservation of angular momentum, as ocean tides redistribute mass and currents move in relation to the solid Earth; (2) external tidal torques from the motion (chiefly) of the Moon and Sun (Chao and Ray, 1997). Tidal forces have been suggested to produce changes in the Earth's rotation and millisecond-scale variations in the length of day (LOD) (e.g. Lambeck, 1980; Brosche *et al*., 1989; Yoder *et al*., 1981). Rotational or LOD changes have been associated with atmospheric variability in zonal winds and circulation patterns (Munk and MacDonald, 1960; Lamb, 1972; Lambeck, 1980), and with fluctuations in angular momenta of the Earth's atmosphere and mantle (Hide *et al*., 1980). Rotational and LOD variations have been related to climate oscillations. For example, connections have been made to the climate-related 40 day intra-seasonal wave (Madden and Julian, 1971) by Langley *et al*. (1981) and Eubanks *et al*. (1985), and to the quasi-biennial oscillation (QBO) and SOI by Dickey (1993); see also Eubanks (1993).

Building on work by Doodson (1921) and others, Cartwright and Tayler (1971) computed the gravitational tidal potential, the principal terms of which were expressible as a combination of six fundamental components. Wood (1986) and Cartwright (1974) derived luni-solar cycles with periodicities of up to millennia (e.g. see Wood (1986), tables M and N).

The total tidal power available from the Sun and Moon is 3.7 TW, and provides more than half the power needed for vertical mixing in the ocean (Munk and Wunsch, 1998). From this analysis of tidal energy flux, Keeling and Whorf (1997, 2000) proposed a mechanism in which luni-solar tidal periodicities generate climate effects through the periodic upwelling of cold water and variability in SSTs. This process was invoked to explain approximately 6 and 9 year SST oscillations (Keeling and Whorf, 1997). It was also used to explain millennial-scale temperature-related sedimentary data in terms of a tidal cycle with a period of 1800 years (De Rop, 1971), the return time for near coincidence of events in the 5.997 year perigean eclipse cycle (Keeling and Whorf, 2000).

Shaffer and Cerveny (1998) find extreme equilibrium ocean tides corresponding to luni-solar alignment periodicities of about 10, 100 and 400 millennia that are probabilistically related to coastal impacts. Cerveny and Shaffer (2001) show a statistically significant association of the 18.6 year lunar nodal cycle with SSTs in the 'Cold Tongue' region of the Pacific Ocean (see http://tao.atmos.washington.edu/data_sets/cti/) and with the SOI. At greatest lunar declination, tidal forces are maximized (Burroughs, 1992), and Cerveny and Shaffer (2001) speculate, following O'Brien and Currie (1993), that the induced changes in winds and temperatures are amplified by changes in the angular velocity of the solid Earth.

Brier (in Lamb (1972): vol. 1; 220) suggested that periodicities of 13.6, 27.2 and 44 years should appear in meteorological data, due largely to tidal effects from lunar synodic and anomalistic monthly cycles. A synodic month is the interval between successive New Moons, and an anomalistic month is the interval between times of successive perigee (the smallest Earth–Moon distance in a lunar orbit). Both in Lamb (1972) and in Burroughs (1992), it was noted that Brier's periodicities are not prominent in meteorological time series. Brier attached importance to the simultaneous completion of whole numbers of luni-solar cycles, and also to half- or whole-year cycles. The method described below, following Brier's idea of simultaneity, may succeed in reproducing some of his results, and examines its possible climate consequences on shorter time scales.

The physical and mathematical approach in this paper does not lead to a qualitative distinction between processes operating over the different time descriptors used in the climatology literature (inter-annual, decadal, inter-decadal, multi-decadal, and so on). So, for simplicity, periodicities between 1 and 10 years will be called 'sub-decadal' and those between 10 and 100 years 'super-decadal'.

2. METHODS

To compare tidal and climate oscillation data, accurate time series analysis is required. Conventional Fourier software may manipulate data (appending a data set to itself, or adding zeros to reach a required data length), or be unable to provide solutions from a continuous or from a selected range of possibilities, or be unable to allow some cycle parameters to be fixed. To avoid such limitations, time series analysis software was written to find components in climate time series data. Data were assumed to be the sum of components $A\cos[2\pi(t-t_0)/P]$, where A is the amplitude, P the period of the cycle, t the time, and t_0 a reference time. The phase angle is then $2\pi(t-t_0)$. In exploratory work, t_0 was simply the time at the beginning of the data to be analysed. The analytical procedure determined the values of A, P and phase angle that explained most variance as the period, amplitude and phase angle were each varied incrementally. The process was iterated, by re-analysing with smaller increments around this solution, to converge to a more accurate solution. Solutions for the three variables could thus be found over an essentially continuous range. When required, a second cycle was found in the residuals, and so on. Later time series analysis fixed t_0 and P in order to test phase angle or other relationships. A circumstantial check on the accuracy of this approach is to be found in the remarkable agreement with the timing of physical events, as will be described.

Attempts to link data to physical events are often limited to establishing coincidence in periodicity. However, coincidence in timing is also crucial for the attribution of causality, so phase angles are converted below to times of cycle maxima for comparison purposes.

Algorithms (Meeus, 1991) were encoded to provide accurate positions of the Sun and Moon at 0 hours UT for every day from the beginning of AD 1866, the start of the reconstructed SOI record. The combined tidal effects of the Sun and Moon were then derived. Mean monthly values of the total tidal force were obtained from daily values, and used in the time series analysis. There were four reasons for the choice of monthly values:

(1) the statistical software was incapable of handling the 30-fold greater data array of daily data;
(2) AD 1866–2000 SOI data are available only as mean monthly data, and it seemed appropriate to analyse SOI and tidal data over the same time intervals;
(3) the modulation of tidal data against the calendar month conferred an important advantage in widely separating the contributors to the time-variation of the data, as described below, while still allowing the underlying short-period cycles to be identified;
(4) the use of monthly data may test Brier's idea of the significance of 6- and 12-monthly intervals.

3. FORCES IN THE PLANE OF THE MOON'S ORBIT

Time series analysis of luni-solar tidal force in this plane produced major components with periods 1.1273, 2.7158 and 0.7965 years. The sum of the reciprocals of the first two periods is virtually identical to the reciprocal of the third. Such 'frequency demultiplication' occurs in non-linear systems (Tsien, 1954). The first, equal to 411.78 days, may be ascribed (Yoder *et al.*, 1981) to the coupling of synodic and anomalistic cycles, and is the evectional period in the Moon's parallax (Wood, 1986: 319).

The second two may be 'pseudo-periods' from the modulation of lunar cycles with the mean calendar month. The period P of an underlying cycle in days is given by $P = M(12y-1)/12y$, where M is the mean length of a calendar month (365.2422/12 days) and y the pseudo-period in years. The underlying cycles for the two pseudo-periods are thus 29.504 and 27.253 days, similar to the lunar synodic (29.530 59) and anomalistic (27.554 55) months. Modulating the underlying cycles against a calendar month was an effective technique to resolve two narrowly separated cycles, the pseudo-cycle periods derived from time-series analysis being separated by years not days.

The mean calendar month is slightly longer than these lunar months. If a maximum in daily tidal force occurs in the middle of a calendar month, the extra days at the beginning and end of the month will have relatively low values in daily tidal force. This results in a *minimum* in the time dependence of the

mean *monthly* tidal force for the pseudo-cycle. Thus tidal maxima are sought at 270° phase angles in the 0.8–2.7 year sine cycles. Pursuing Brier's idea on the coincidence of synodic and anomalistic periods, it should be noted that the 1.1273, 2.7158, and 0.7965 year tidal maxima coincide at 1920.46. Since the three periods are almost exact sub-multiples of 59.75 and 13.53 years, the times of coincidence over the period AD 1866 to 2040 display these intervals (Figure 1). Figure 1 was generated using a slightly adjusted third period of 0.7966 years, to be internally consistent with frequency demultiplication. The frequency demultiplication relationship means that a combination of any two of the three 0.8–2.7 year cycles effectively generates a similar pattern of maxima. Wood (1986: table N) shows periodicities of 13.502 and 59.750 years, in a list of 136 tidal cycles with periods between about 1 and 40 000 years, that create maximized gravitational forces on Earth.

Largely because of the presence of the Sun, the Moon's elliptical orbit around the Earth does not have a constant shape or orientation, but changes continuously. For any particular lunar orbit, perigee distance can range from about 357 000 to 370 000 km, and perigee near the former distance is designated herein as 'close perigee' (Figure 2). Events in Figure 1 correspond remarkably well to the near-coincidence of New Moon and close perigee (Table I). This agreement lends support to the time series analysis. Some events occur at a time flanked by close New Moon configurations. On these occasions the central time is close to Full Moon with an apogee exceeding 406 400 km (see http://www.fourmilab.com/earthview/pacalc.html). (Apogee distance varies from about 404 000 to 406 700 km (Meeus, 1991)).

Time series analysis of SOI data between AD 1866 and 2000 produced two main super-decadal cycles with periods of about 13.5 and 45 years, reminiscent of Brier's suggestion noted earlier. There are suggestions of an approximately 13 year cycle in the climatology literature (e.g. Navarra, 1999; note the articles by Folland *et al*. (1999), Latif (1999), and Mysak (1999)).

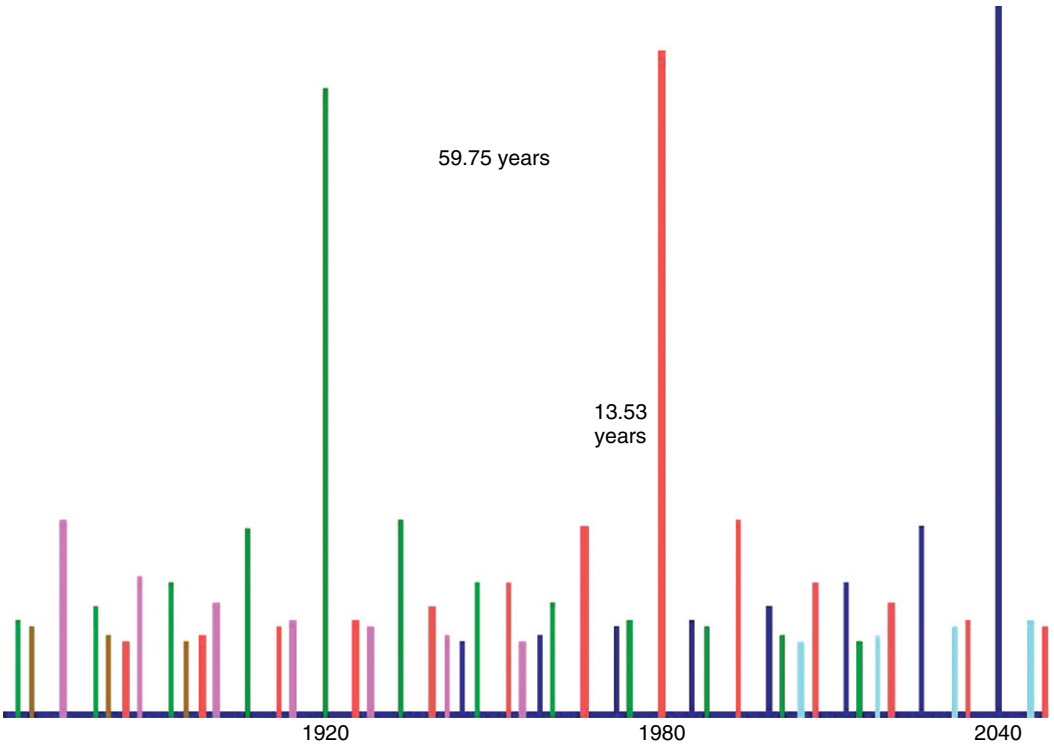

Figure 1. The pattern of tidal events from 1866 to 2050. The height of each bar is inversely proportional to the square root of the time interval covering the three tidal maxima, and so is related to the interval (http://www.fourmilab.com/earthview/pacalc.html) between close perigee and New Moon. The repeated feature, differentiated by colour, is a bell-shaped envelope of 13.53 year spacings, with the centres of the envelopes separated by 59.75 years. By locating one event in time (for example 1920.46), all events are located in time

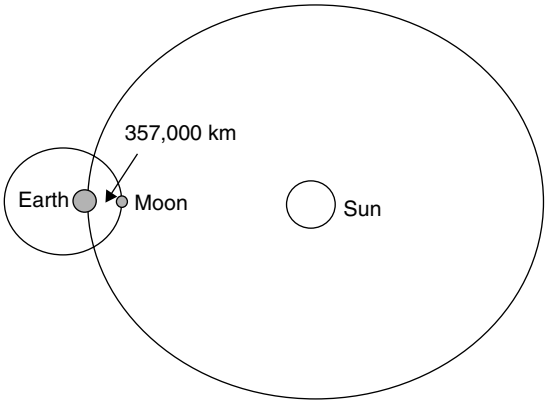

Figure 2. Coincidence of New Moon with close perigee

Figure 1 shows phase-shifted envelopes of 13.53 year cycles. If 13.53 year tidal events drive the SOI, the correspondence should be most clear for SOI data over times within one tidal envelope. Analysis of overlapping multi-decadal sets of SOI data suggests that events under each 60 year tidal envelope require about half a cycle to be established over the previous (phase-shifted) series. For example, a regression of the monthly amplitudes of a cycle, with maxima at $1920.46 + 13.53n$, against monthly 1920–79 SOI data produces a t statistic of +3.7. A Monte Carlo simulation, in the form of randomly varying phase angle, and randomly varying cycle period between 10 and 100 years, indicates that a t statistic of this absolute magnitude would occur only about three times in 1000 by chance. It is suggested that a phase-shifted tidal cycle does not overcome and dominate the climate response to the preceding phase until after the biggest tidal 'spike' has been reached in the new phase, and this suggestion will be applied again later.

The 45 year cycle maxima also coincide closely with major tidal events at $1920.46 + 46.22n$ (Figure 3). A regression of the monthly amplitude of a hypothetical 46.22 year cycle having these times of maxima, against AD 1866–2000 monthly SOI data, produces a t statistic of +5.3. A Monte Carlo simulation, varying phase angle (timing) randomly, and varying cycle period randomly over the 10–100 year super-decadal range, indicates that a t statistic having this absolute value would be reached in only about two times in 1000 by chance.

One might have expected to find a cycle of length 59.75 years rather than 46.22 years, and an explanation will be offered toward the end of Section 4. In any event, the 59.75 year tidal cycle may exhibit its presence in climate circulation patterns. The Earth's rotational acceleration has been used to define different atmospheric circulation regimes (Lamb, 1972), and shows a 60 year cycle with maxima near 1860 and 1920 (Lambeck, 1980). This variability is similar in profile to the envelope of tidal forces in Figure 1, at least up to about 1950.

The preceding suggests that tidal maxima in the plane of the Moon's orbit coincide with super-decadal SOI maxima, and therefore that the primary responses are La Niña-like events. This is consistent with the suggestion (Keeling and Whorf, 1997) that tidal forces produce upwelling and cool SSTs. El Niño events may be consequences of these perturbations, possibly linking with relaxation or oscillatory processes characterized by the ocean–atmosphere system (Schopf and Suarez, 1988; Neelin *et al*., 1998). Another possible contributor to El Niño is described later.

Why tidal forces in the plane of the Moon's orbit produce a response in the SO, and not in some other oscillation, may perhaps be answered conceptually with the geometry of Figure 2. The Moon's orbit is nearly coplanar with the plane of the Earth's orbit around the Sun (the ecliptic). The 23.5° inclination of the Earth's rotational axis to the ecliptic defines the tropical zone. Thus, as the bodies move and the Earth rotates on its axis, the radius vector sweeps chiefly between the tropics — producing a response manifested in a zonal equatorial phenomenon such as the SO.

Table I. Events involving coincidence of New Moon with close perigee, with tidal forces in the plane of the Moon's orbit[a]

Decimal date from analysis	Equivalent date	Nearest tidal event	Perigee distance (km)	Displacement from New Moon (h)
1860 series				
1860.71	17 Sep 1860	15 Sep 1860	357 022	2
1874.24	28 Mar 1874	18 Mar 1874	357 070	6
		15 Apr 1874	357 812	−14
1887.77	8 Oct 1887	16 Oct 1887	356 920	−4
1901.30	19 Apr 1901	18 Apr 1901	357 096	0
1914.83	30 Oct 1914	19 Oct 1914	357 108	9
		17 Nov 1914	357 221	−12
1928.36	12 May 1928	20 Apr 1928	357 734	14
		19 May 1928	357 419	−6
1941.89	21 Nov 1941	19 Nov 1941	356 675	1
1920 series				
1906.93	5 Dec 1906	17 Nov 1906	357 695	16
		15 Dec 1906	356 743	−4
1920.46	18 Jun 1920	16 Jun 1920	357 255	1
1933.99	27 Dec 1933	17 Dec 1933	356 944	9
		15 Jan 1934	357 245	−12
1947.52	8 Jul 1947	17 Jul 1947	357 307	−4
1961.05	19 Jan 1961	16 Jan 1961	356 677	1
1974.58	30 Jul 1974	19 Jul 1974	357 518	8
		17 Aug 1974	357 585	−11
1988.11	10 Feb 1988	19 Jan 1988	357 511	15
		17 Feb 1988	356 914	−6
2001.64	21 Aug 2001	19 Aug 2001	357 158	2
1980 series				
1966.67	1 Sep 1966	14 Sep 1966	357 045	−2
1980.21	18 Mar 1980	17 Mar 1980	356 927	1
1993.74	27 Sep 1993	16 Sep 1993	357 404	11
		15 Oct 1993	357 241	−10
2007.27	8 Apr 2007	17 Apr 2007	357 137	−5
2020.80	20 Oct 2020	16 Oct 2020	356 912	4
2034.33	30 Apr 2034	19 Apr 2034	357 337	8
		17 May 2034	357 643	−12
2047.86	10 Nov 2086	17 Nov 2047	356 787	−2
2061.39	22 May 2061	19 May 2061	357 186	1

[a] Data in the last three columns from http://www.fourmilab.com/earthview/pacalc.html.

4. FORCES PERPENDICULAR TO THE PLANE OF THE MOON'S ORBIT

To test this hypothesis, tidal forces in the plane *perpendicular* to the Moon's orbit were determined, to see if the orthogonal pattern resembles super-decadal features in a meridional or mid-latitude phenomenon such as the IPO (e.g. Power *et al.*, 1999). Time series analysis of tidal forces in this plane produces major components with periods 0.70 and 6.00 years. The latter may be assignable to the 5.997 year perigean eclipse cycle, which is also the beat period between the anomalistic and nodical months (Keeling and Whorf, 1997). One can examine the beating together of these two mid-latitude and the three equatorial (0.8 to 2.7 year)

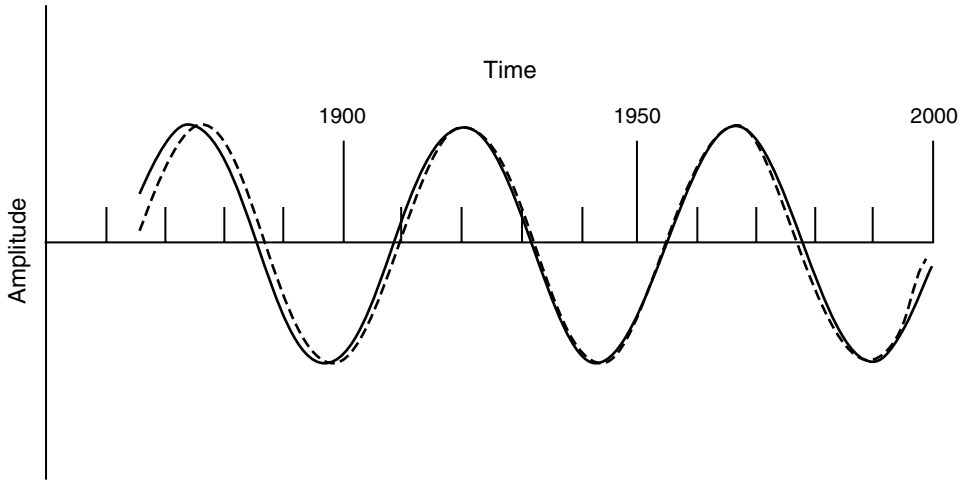

Figure 3. Comparison of 46 year tidal (solid) and SOI (dotted) cycles. The SOI cycle has maxima at $1921.25 + 45.0n$ (1876.25, 1921.25, and 1966.25). Major tidal events occur at 1874.24, 1920.46, and 1966.68, spaced 46.22 years apart, and a sine cycle with maxima at these tidal events is shown. The greatest amplitudes of the two sine waves are set equal for comparison. The SOI and tidal cycles match to about 2.6% in period and 1.8% in phase angle. (In subsequent figures, the timing of tidal events and climate cycle maxima are indicated by vertical lines rather than by hypothetical sine waves)

cycles. The pairs that produce beats that are both regular and strong (in terms of virtually simultaneous maxima) are the pairs with periods 0.70 and 1.1273, 6.00 and 1.1273, and 0.70 and 0.7966 years.

Coupling the 0.70 and 0.7966 year cycles produces sequences of three cycles of 5.588 years followed by a cycle of 6.336 years, for a continuous and fairly regular mean period of about 5.775 years. A major event occurs for this pairing in 2039.96. In a simple regression of the monthly amplitude of this cycle against unfiltered monthly 1875–2000 UKMO SST data, a t statistic of $+10.3$ is produced. A Monte Carlo simulation, varying the phase angle randomly, and varying the period randomly over the sub-decadal range (1 to 10 years), indicates that a t statistic with this absolute value occurs only about four times in 1000 by chance.

Coupling the 0.70 year cycle with the 1.1273 year equatorial cycle produces three phase-shifted envelopes since AD 1860. The main tidal maxima are spaced 86.795 years apart at 1866.37, 1953.165, and 2039.96, with a family of events spaced $20.295n$ years around these events, all associated with near-coincidence of New Moon and close perigee. These times are listed in Table II, and once more show the tidal time series analysis closely matching major physical events. Wood (1986: table N) shows periodicities of 20.294 and 86.834 years, in a list of 136 tidal cycles with periods between about 1 and 40 000 years, that create maximized gravitational forces on Earth.

Since equatorial Pacific SSTs are inversely correlated with the SOI, the IPO pattern should be inverted to correspond with the tidal–SOI pattern. From time series analysis of the band-filtered three-monthly IPO data from AD 1900 to 1999, maxima in a major component occur at $1951.99 \pm 19.95n$, corresponding closely to the 20.295 year tidal periodicity (Figure 4). Analysis of the IPO data over the 1856–2000 period shows component maxima at $1958.4 \pm 85.7n$, in reasonable agreement with tidal 86.795 year cycles having maxima at 1953.165 suggested earlier. The above hypothesis, that climate cycles are directionally determined by orthogonal moments of the tidal force, seems to survive. Fixing periods and phase angles at the tidally determined values, the 86.795 and 20.295 year cycles together account for about 35% of the variance in the three-monthly low-pass filtered IPO data, and about 8% of the variance in the unfiltered monthly UKMO data.

The 86.795 and 20.295 year cycle contributions to the unfiltered UKMO SST data provide about twice the variance of the 46.22 and 13.53 year cycle contributions to the SOI. A regression of the 86.795 year cycle in the unfiltered 1856–2000 UKMO data produced a t statistic of -9.4, and a regression of the 20.295 year cycle in the unfiltered AD 1900–2000 UKMO data produced a t statistic of -7.8. Monte Carlo simulations,

Table II. Events involving coincidence of New Moon with close perigee, with tidal forces perpendicular to the plane of the Moon's orbit[a]

Decimal date	Equivalent date	Nearest tidal event	Perigee distance (km)	Displacement from New Moon (h)
1866 series				
1866.37	14 May 1866	14 May 1866	357 291	−5
1886.665	30 Aug 1886	29 Aug 1886	357 279	−3
1906.96	16 Dec 1906	15 Dec 1906	356 743	−4
1953 series				
1871.985	25 Dec 1871	12 Dec 1871	357 160	10
		10 Jan 1872	357 163	−11
1892.28	13 Apr 1892	28 Mar 1892	357 255	9
		26 Apr 1892	357 648	−12
1912.575	30 Jul 1912	14 Jul 1912	357 520	10
		12 Aug 1912	357 498	−10
1932.87	14 Nov 1932	30 Oct 1932	357 210	11
		27 Nov 1932	357 007	−10
1953.165	1 Mar 1953	14 Feb 1953	357 107	9
		14 Mar 1953	357 409	−12
1973.46	17 Jun 1973	1 Jun 1973	357 577	9
		30 Jun 1973	357 768	−11
1993.755	2 Oct 1993	16 Sep 1993	357 404	11
		15 Oct 1993	357 241	−10
2014.05	19 Jan 2014	1 Jan 2014	356 921	10
		30 Jan 2014	357 079	−11
2039 series				
1979.075	28 Jan 1979	28 Jan 1979	356 740	3
1999.37	15 May 1999	15 May 1999	357 096	2
2019.665	30 Aug 2019	30 Aug 2019	357 175	4
2039.96	16 Dec 2039	15 Dec 2039	356 817	4

[a] Data in the last three columns from http://www.fourmilab.com/earthview/pacalc.html.

randomly varying phase angle, and randomly varying cycle period between 10 and 100 years, indicate that the absolute values of these t statistics are respectively reached in about 70 and 160 cases in 1000 by chance.

The 20.295 year mid-latitude cycle may be an alternative to the 18.6 year lunar nodal and 22 year solar magnetic cycles in answering the 'formidable' (Burroughs, 1992) case for a 20 year meteorological cycle; see also Hibler and Johnsen (1979). Such a cycle should not be 'written off' as an average of cycles having periods of 18.6 and 22.4 years (Fairbridge and Sanders, 1987). The timing of tidal events in Table II and Figure 4, including the phase shifting of 20.295 year cycles between 'parent' 86.795 year maxima, is at least superficially similar to the timing of EOF maxima in temperature and precipitation data in Latif and Barnett (1996) and articles in Navarra (1999).

Coupling the 6.00 and 1.1273 year cycles produces phase-shifted cycles with intervals of 18.02 years. There are ten consecutive 18.02 year events followed by a 5.82 year phase shift, followed by another ten events separated by 18.02 years, and so on. Averaging this behaviour over ten intervals, the mean interval is 18.6 years, and so we seem to connect the saros (more accurately 18.030 years in length) with the 18.6 year lunar nodical cycle.

This apparent connection may be worth pursuing. The beating of the 6.00 and 1.1273 year cycles produces the highest tidal spike in the 20th century at 1918.22. Following the earlier suggestion involving the 13.53 year cycle, we provisionally take this to be when the new phase supersedes the previous phase, in its influence on climatology. Thus, the phase-shifted 18.02 year cycle may produce maxima in climate response after 1918 at

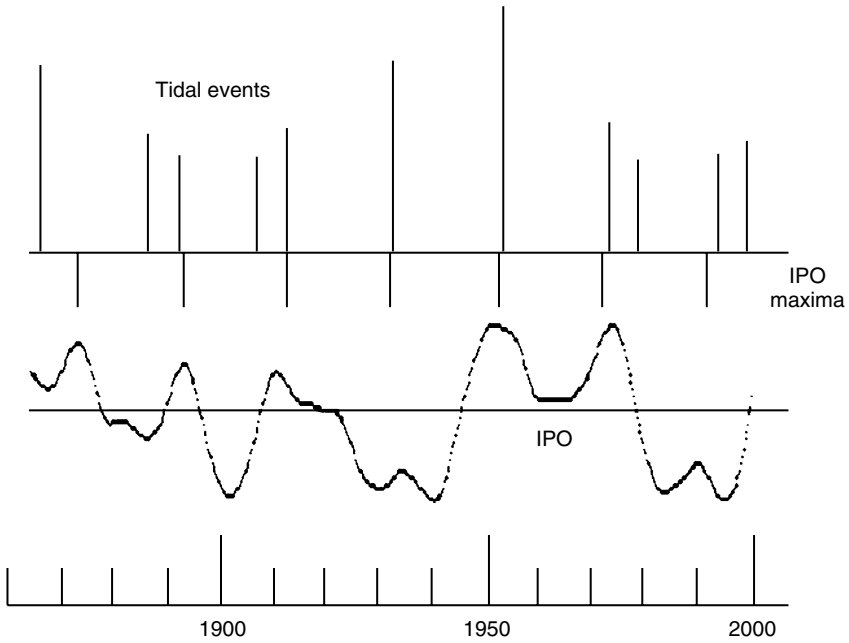

Figure 4. Mid-latitude tidal force and the IPO from 1860 to 2000

1918.22, 1936.24, 1954.26, 1972.28, 1990.30, and so on, whereas prior to 1918 the climate parameters may respond to the late stages of the preceding phase with events at 1912.40, 1894.38, 1876.36, and so on. Given this interpretation, the 18.02 year cycle has maxima in approximately the same positions as some examples of climate response to the 18.6 year cycles derived by Currie and co-workers (e.g. Currie, 1987; O'Brien and Currie, 1993; Currie and Vines, 1996). This clearly does not explain all examples, but conceivably phase-shifted 18.02 and 20.295 year cycles may offer a partial answer to the results cited in these papers. See Keeling and Whorf (1997) for overlapping sequences of 18.030 year tide raising cycles, based on Wood (1986).

Cerveny and Shaffer (2001) place 18.6 year tidal maxima at maximum lunar declination, which occurs at about $1950.5 \pm 18.6n$. Currie and co-workers (Currie, 1987; O'Brien and Currie, 1993; Currie and Vines, 1996) place tidal maxima at $1954.7 \pm 18.6n$. The difference of about 4 years is presumably a result of the latter's inclusion of the solar tide, a point made explicit in Currie (1987). The similarity in timing of Currie's maxima with the post-1918 18.02 year maxima found in the present study may be at least partly attributable to the common luni-solar approach.

One can test the presence of various 18 year cycles in the unfiltered UKMO monthly 1856–2000 SST data, before and after 1918, by a simple regression of monthly tidal amplitudes against the monthly SST data. The cycle given by Cerveny and Shaffer (2001) produces t statistics of -6.66 and -3.75 for regression against pre- and post-1918.0 SST data respectively. The cycle adopted by Currie and co-workers (Currie, 1987; O'Brien and Currie, 1993; Currie and Vines, 1996) produces t statistics of $+0.57$ and -3.97 for pre- and post-1918.0 SST data. In the present paper, the pre-1918 phase of the 18.02 year cycle produces a t statistic of -7.62 with pre-1918.0 SST data, and the post-1918 phase of the 18.02 year cycle produces a t statistic of -4.75 with post-1918.0 data. Monte Carlo tests with cycle periods selected randomly between 10 and 100 years, and with randomly selected times of maxima, show that none of the post-1918.0 t statistics are unusual. However, in the pre-1918.0 cases, the -6.66 and -7.62 t statistics (as their absolute values) are respectively reached only about 16 and 4 times in 1000 by chance.

Most of the t statistic signs are negative, consistent with tidal forces producing upwelling and sea surface cooling (Keeling and Whorf, 1997). Currie (1987) explained pre-1918 results by a phase shift in his 18.6 year cycle. The present paper includes a solar tidal effect, incorporates an explicit phase shift in climate response

around 1918 (if the argument based on the 13.53 year cycle is accepted), and generates t statistics that are comparatively significant.

5. HYPOTHETICAL SUB-DECADAL COMPONENTS

The sub-decadal 5.775 year cycle is derived directly from tidal considerations above. Although this cycle has a statistically supported presence in climate oscillations, a wide range of sub-decadal components is needed to reproduce the sub-decadal variability of these oscillations. A speculative attempt is made in this section to address this issue.

The agreement above between tidal and super-decadal components in the SOI and IPO suggests that the time series analyses are accurate. However, the amplitude of the SOI often exceeds 30 units, whereas each of the two SOI cycles of 13.53 and 46.22 years have amplitudes of only two units and contribute only about 2% of the variance. The agreement in timing seems too good, if random or non-tidal processes cause the other (sub-decadal) components in the SOI. However, the agreement might be explained if sub-decadal components are also generated from the same tidal processes.

Recalling the equatorial tidal pattern, major tidal maxima occur at intervals of 59.75 years, with phase-shifted maxima at intervals of 13.53 years. The only tide-generated short-period cycles that would produce a sustained SO response are cycles that are continuous, not phase shifted or interrupted. These cycles would need to avoid destructive interference and to coexist in the presence of major tidal cycles of 59.75 and 13.53 years. A class of such 'survivors' contains cycles with periods near whole-number sub-multiples of 59.75 and 13.53 years, and with maxima that coincide with major tidal maxima (e.g. 1920.46). In the sub-decadal range, such cycles have periods 1.127, 1.219, 1.494, 1.707, 1.927, 2.213, 2.298, 2.716, 4.596, and 6.639 years (Table III). These periods are whole-number sub-multiples of 59.75 years, and close to whole-number sub-multiples of 13.53 years. If one such cycle reaches maximum at 1920.46, it will also reach maxima at 1980.21 (the next major maximum) and at close to the intervening 13.53 year intervals. In this circumstance, it is speculated that the sub-decadal cycle may have long-term stability.

Some of these sub-decadal cycles, and cycles derived elsewhere in this paper, are similar in length to known terrestrial oscillations (for example, the QBO), but such speculative attributions cannot be pursued here.

Other possible members of this group were excluded if the ratios $59.75/P$ and $13.53/P$ were both even, because the 59.75 and 13.53 year maxima would then coincide with P minima as well as P maxima, and the P cycle should not be stabilized. The only such cycle included is the 2.2981 year cycle, with ratios of 26 and about 6, which makes an important contribution (amplitude two units) to the SOI. Selection rules for admission or rejection are not understood at this stage.

Table III. Times of maxima of 59.75 and 13.53 year sub-multiple tidal components present in SOI data, compared with the tidal 1920.46 maximum (designated t_0 here). The values of t were derived from time series analysis of SOI data

Period P (years)	$59.75/P$	$13.53/P$	1920 year maximum t	Abs$(t - t_0)$ Δ (years)	Out of phase $100\Delta/P$ (%)
1.1274	53	12.00	1920.39	0.07	6.2
1.2194	49	11.10	1920.61	0.15	12.3
1.4938	40	9.06	1920.53	0.07	4.7
1.7071	35	7.93	1920.59	0.13	7.8
1.9274	31	7.02	1921.15	0.69	35.5
2.2130	27	6.11	1920.46	0.00	0.0
2.2981	26	5.91	1920.35	0.11	4.8
2.7159	22	4.98	1920.35	0.11	4.1
4.5962	13	2.94	1921.11	0.64	13.9
6.6389	9	2.04	1923.20	2.74	41.3

To test the presence of the hypothesized sub-decadal cycles in climate variability, time series analysis was carried out on AD 1866–2000 SOI data. Component periods were now *fixed* at each of the ten tidally derived values in turn, but amplitude and phase angle were allowed to vary. Eight of the ten SOI sub-decadal components extracted show a maximum shifted between −5 and +14% in phase from the 1920.46 tidal maximum (Table III). The likelihood of this result occurring by chance is one in several hundred, consistent with a response to luni-solar tidal forces.

Some of the longer sub-decadal cycles show considerable phase shifts (last column of Table III) with respect to the 1920.46 maximum.

Sub-multiple ratios R of $59.75/P$ or $13.53/P$, related as $R_1 = R_2 + R_3$, are evidence for frequency demultiplication, and there are examples in Table III. For example, the 1.4938 year cycle could be generated from the pair 2.213 and 4.5962. (The period ratios in columns 2 and 3 are simple sums.) The 2.2981 year cycle might be pruned from the list on the grounds that it may be an overtone of the 4.5962 year cycle. The 2.2130 year cycle might be excluded because it may be an overtone of the 6.6 year cycle. The 6.6 year cycle is virtually identical to a cycle listed in Table IV later, and may more appropriately belong to that list.

When several of the derived sub-decadal SOI components are appropriately combined, the composite resembles the tidal pattern. For example, when the 1.127 and 2.716 year components are added together (Figure 5), spacings of 59.7 and 13.5 years occur between the main maxima. The ten greatest maxima occur at times virtually identical to tidal maxima of Figure 1, with a mean difference of only 0.07 years. It needs to be emphasized that the timing of these maxima were found by time series analysis of the SOI, and that this timing coincides with that found by an independent time series analysis of the tidal force. Not only does the combination of the two components in the SOI accurately reproduce the timing of the tidal events, it also reproduces the 13.53 year phase shift. This result seems to lend support for the presence of tidal influences in the SOI.

It might be suggested that the improbable sub-decadal coincidences noted might not be unlikely if cycles are related by frequency demultiplication. However, such an explanation implies a connection with the periods 59.75 and 13.53 years, which only reaffirms the link with tidal events. Overall, the period and timing of many super- and sub-decadal SOI components, singly or combined, mirror the tidal stimulus. This implies that the variability of the SO is at least partly influenced by tidal forces from the Sun and Moon.

The ratio 20.295/13.53 is exactly 1.5, so there are two and three cycles respectively in 40.59 years, suggesting the possibility of coupling or resonance between equatorial and mid-latitude oscillations.

A test of this is to see if sub-multiples of the main *mid-latitude* periodicities (86.795 and 20.295 years) are also present in the (equatorial) SOI. Examples of these sub-multiples are cycles with periods 1.5499, 1.7019, 1.8467, 2.0185, 2.2841, 2.8932, 4.1331, 5.1056, 6.6765, and 9.6439 years, generated with the criteria used in Section 4. As before, time series analysis was carried out with sub-multiple cycle periods fixed while

Table IV. Times of maxima of 86.795 and 20.295 year sub-multiple mid-latitude tidal components present in SOI data, compared with the tidal 1953.165 maximum (designated t_0 here). The values of t were derived from time series analysis of SOI data

Period P (years)	$86.795/P$	$20.295/P$	1953 year maximum t	Abs$(t - t_0)$ Δ (years)	Out of phase $100\Delta/P$ (%)
1.5499	56	13.09	1953.80	0.64	41.1
1.7019	51	11.93	1953.01	0.15	8.9
1.8467	47	10.99	1952.56	0.61	32.9
2.0185	43	10.05	? (A ≈ 0)	—	—
2.2841	38	8.89	1952.25	0.91	40.1
2.8932	30	7.01	1953.55	0.38	13.2
4.1331	21	4.91	1955.21	2.04	49.4
5.1056	17	3.98	1954.63	1.47	28.8
6.6765	13	3.04	1956.09	2.93	43.8
9.6439	9	2.10	1948.44	4.73	49.0

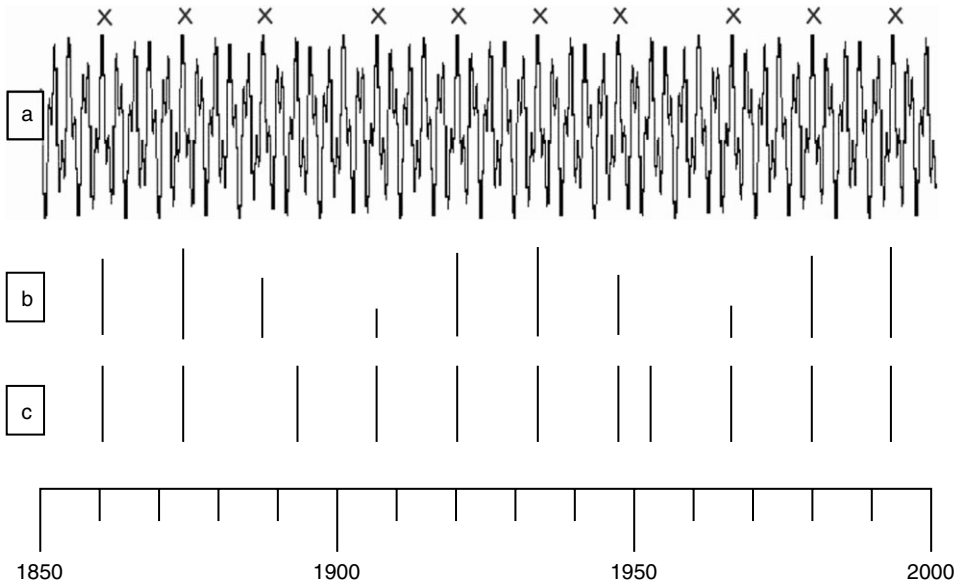

Figure 5. The combination of two SOI components derived from time series analysis. The periods were fixed at the tidal values of 1.127 and 2.716 years, but phase angles (timing) and amplitudes were allowed to vary: (a) the sum of the two SOI cycles; (b) the timing and amplitude of the major SOI peaks, marked as X in (a) — amplitude differences are greatly exaggerated; (c) the timing in the tidal pattern of Figure 1, for comparison

amplitudes and phase angles were varied. The results in Table IV show the shift in maxima from the main mid-latitude tidal component at 1953.165. Several of the phase shifts in the last column are close to 50%. This suggests that the mid-latitude components in the SOI tend to 'avoid' being in phase with the 1953.165 mid-latitude tidal maximum.

There are several potential non-linear (frequency demultiplication) interactions here. For example, the 1.8467 year cycle may be generated non-linearly from the pair 2.8932 and 5.1056. (The period ratios in columns 2 and 3 are simple sums.) The 1.7 year cycle might be pruned from this list on the grounds that it appears to be an overtone of the 5.1 year cycle, and that it is virtually identical to a cycle in Table III.

One can test whether this anti-phase relationship at 1953.165 is unusual. For any time, the combined absolute shifts in phase $\Sigma(\Delta)$ can be found for the set of cycles in Table IV. Between AD 1850 and 2000, the greatest $\Sigma(\Delta)$ values are found at 1866.34, 1885.74, 1932.84, 1953.14, and 1972.54. The close similarity of these times to maxima in Table II is obvious, and the strong anti-phase relation between this family of sub-decadal SOI components and mid-latitude tidal events seems clear. Whereas equatorial tidal maxima may be associated with La Niña tendencies (earlier), mid-latitude tidal maxima appear (through their anti-phase relationship with the SOI) to be associated with El Niño tendencies.

In sum, there may be two distinct classes of sub-decadal SOI cycles. The first class contains sub-multiples of major equatorial tidal periodicities, with timing in phase with their maxima (e.g. 1920.46); these might be characterized as zonal equatorial cycles. The second class contains sub-multiples of major mid-latitude tidal periodicities, with timing in anti-phase with their maxima (e.g. 1953.165); these might be loosely characterized as mid-latitude, extra-tropical or meridional cycles. Whether these two classes exhaust the possibilities is unknown.

6. THE COMBINATION OF ORTHOGONAL COMPONENTS

The SOI can apparently be represented in part as a composite of equatorial and mid-latitude sub-decadal components. As mentioned previously, the SOI is correlated with unfiltered Pacific SST parameters, which

implies that these parameters are also, in part, composites of tidal sub-decadal components. One may now return to the super-decadal range, and ask if there is an indication of combined contributions there.

As we have seen, super-decadal events are characterized by intervals of $59.75 + 13.53m$ and $86.795 + 20.295n$ years, for equatorial and mid-latitude cases respectively. As m and n are varied (positive and negative), common solutions arise at intervals of 40.59 years: 5.62, 46.2, 86.8, 127.4, 168.0, and 208.6 years, and so on. Recall that a 46.22 year analogue is seen in the SOI rather than the 59.75 year cycle that might have been expected from the equatorial analysis. The 46 year SOI periodicity may arise because it is an interval common to both equatorial and mid-latitude components, and so the super-decadal SOI components may also reflect a combination of equatorial and mid-latitude factors.

As a final test of the approach, equatorial and mid-latitude components in Tables III and IV were combined and compared with the SOI. As far as possible, the analytical results were ignored and *ab initio* reasoning used. Table III components were all assumed to have extrema at 1920.46 and the Table IV components at 1953.165. The only analytical result used was a categorical one: the apparent phase relationship of the two sets of components, one in-phase and the other out-of-phase. Components were assumed to have equal amplitudes. If all components from both lists are chosen, the results are similar to those to be described, but frequency demultiplication combinations effectively produce duplication, as explained previously. Components were therefore selected so that a complete list could be reproduced by pair-wise combinations, and with emphasis on the longer cycles to reduce short-period noise for clarity. Thus all members of Table III could be reproduced from pairs of cycles with periods 6.6389 (but using the Table IV equivalent), 4.5962, 2.7159, 2.2981, and 2.213 years. For Table IV, the generating cycles had periods 9.6439, 6.6765, 5.1056, 4.1331, and 2.0185 years. The components were then simply added together. To minimize wide swings in the composite, it was attenuated by using the square root of the absolute value of the amplitude, much as with the tidal pattern in Figure 3. The result of this rather naive combination process is given in Figure 6, with the solid curve representing the composite. There are times of disagreement with SOI data, such as around 1887, 1896, and 1973, and there is some overemphasis on an approximately biennial factor. But, on balance, the linear combination seems to mirror the SOI fairly well, and accurately locates many of the extrema in time.

To examine this point further, the timing of SOI extrema (maxima and minima) may be compared with that of extrema in the SOI tidal analogue in Figure 6. Using a 7 month running mean to smooth monthly SOI data over the period 1866 to 2000, there are 17 SOI extrema with absolute amplitudes greater than 15.0 that lie within 0.25 year, of extrema in the composite of sub-decadal cycles in Figure 6. These SOI–tidal pairs of extrema are in the same direction (both maxima or both minima) in 16 cases, the odd case occurring with 1873 data. Choosing a maximum time difference between extrema of 0.1 years, pairs of extrema match

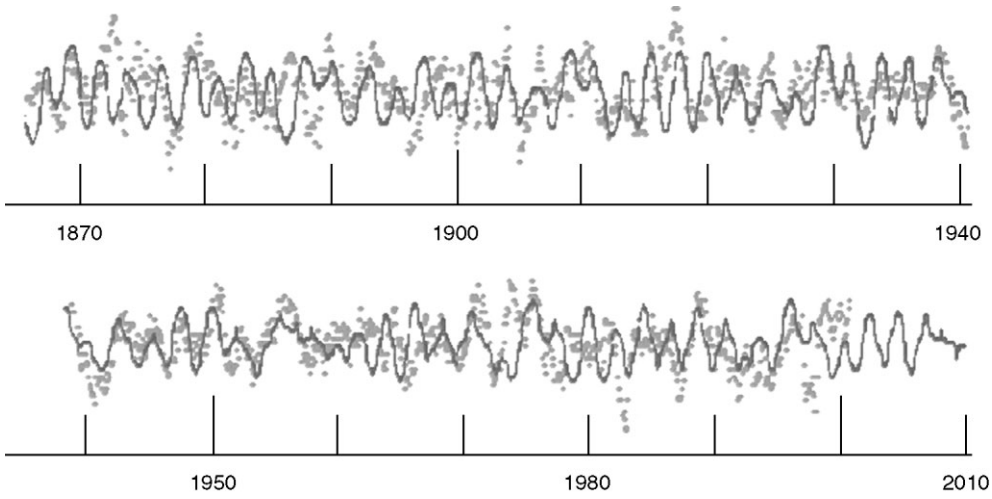

Figure 6. Comparison of a largely theoretical tidally derived oscillation pattern (solid curve) with the SOI (dots). For clarity, the SOI data have been slightly smoothed using a 7 month running mean. The amplitude of the curve was scaled by eye to match the SOI

direction in 11 cases out of 11. The agreement found with such small time differences suggests little or no time lag between the SOI and tidal cycles.

A regression of the monthly SOI data between 1866 and 2000 against the SOI tidal analogue produces a t statistic of +7.0. A Monte Carlo simulation, in the form of the sum of a random set of nine cycles, each with periods between 2 and 10 years, and with random phase angles, shows that a t statistic of this absolute magnitude is reached only about eight times in 1000 by chance.

In the above representation, sub-decadal tidal components do not completely reconstruct the variability of the SO and other climate oscillations with sub-decadal tidal components, but it is suggested that progress may be made in this reconstruction if tidal effects are included in future.

It should be emphasized that this combination is generated on tidal and non-linear considerations, contains little manipulation in the light of SOI data analysis, and naively assumes equal amplitude contributions from the components. The above in-phase and anti-phase relationships might not have been anticipated, but the comparison could otherwise have been produced largely on theoretical grounds. The preceding choice of sub-multiples is not a unique solution, and the 1973 discrepancy (at least) can be corrected with a slightly different set. Incorporating more of the mathematics of interacting non-linear oscillations may improve the regression and the relationship suggested by Figure 6.

7. DISCUSSION

The super-decadal (10 to 100 year) tidal cycles described in this paper have a striking feature in common. With only one exception, and using the sign of the t statistic as an indicator, the timing of tidal maxima coincide with cool SSTs or high SOI values. This is consistent with the promotion of upwelling as mentioned previously. Five cycles fitting this description are the 13.53 and 46.22 year equatorial cycles, and the 86.795, 20.295, and 18.02 year mid-latitude cycles derived herein, as well as the different 18.6 year cycles used by Cerveny and Shaffer (2001) and by Currie and co-workers (Currie, 1987; O'Brien and Currie, 1993; Currie and Vines, 1996). The only exception is the 59.75 year cycle, which has a less significant presence in climate oscillations than the other cycles and with maxima apparently coinciding with warm SST events.

The location of the cool SSTs deserves comment. Results with the equatorial set of super-decadal cycles imply upwelling and cool SSTs near the equator. Results on the mid-latitude cycles are more unexpected, because the phasing or polarity of the IPO SSTs (Power *et al*., 1999) means that the location of cool SSTs is also at the equator and not at mid-latitudes, even though the cycles are notionally 'mid-latitude'. Cerveny and Shaffer (2001) suggest that high lunar declinations (an important factor in mid-latitude tidal cycles, even when including solar tidal influences) increase mid-latitude transport in the ocean and induce cold water advection into the equatorial region.

The sub-decadal tidal cycles also show a clear pattern. The equatorial set tends to have maxima that coincide with cool Pacific SSTs and high SOI values. The mid-latitude set tends to have maxima that coincide with warm Pacific SSTs and low SOI values. The latter is opposite to the mid-latitude pattern for the super-decadal case, and the climate responses of mid-latitude tidal effects may deserve more study.

Even when taken singly, many of the proposed super- and sub-decadal tidal cycles have a significant presence in important climate oscillations. In combination, it seems unlikely that these results could have arisen by chance. The results also suggest the possibility of characterizing to some degree (a) the Earth's natural climate variability and, as a result, (b) anthropogenic effects. It must be borne in mind, of course, that solar radiative and other external factors may additionally contribute to the Earth's natural climate variability.

Since luni-solar tidal processes can be precisely defined centuries in advance, a link with climate variability should lead to improvements in the accuracy of climate forecasting and greatly increase its lead time. Work in progress indicates promise in these areas (Abawi *et al*., 2001). Exploring these ideas further would require collaborative work in astrophysics, geophysics and climatology, and in the particular area of non-linear dynamics including resonant amplification, the process by which small, regular, repeated perturbations produce a noticeable effect.

8. CONCLUSIONS

The temporal variability of the SO and IPO and unfiltered SSTs has been compared with the effects of tidal forces from the Sun and Moon, following and developing ideas proposed by Brier and others. There appear to be multiple tidal contributions over a range of periodicities. The period and timing of five super-decadal (86.795, 46.22, 13.53, 18.02, 20.295 year) tidal cycles appear to have counterparts in climate oscillations. The match between sub-decadal tidal cycles and SOI/SST data also seems notable. When naively combined, the equatorial and mid-latitude tidal components appear to resemble the SOI, and there is statistical support for the presence of tidally generated sub-decadal cycles in the SOI and in SST data. It is hoped that the approach taken in this paper will complement other analyses of tidal effects and analyses based on other possible external drivers of climate effects, such as solar radiative variability.

ACKNOWLEDGEMENTS

Thanks are offered for guidance during the course of this study by Roger Stone, Graeme Hammer, Holger Meinke, Yahya Abawi and others in the Queensland Departments of Primary Industries and of Natural Resources and Mines, and by astrophysicist Brad Carter and statistician Ron Addie of the University of Southern Queensland. Thanks are also offered for constructive comments from Jean Dickey of the NASA Jet Propulsion Laboratories in Pasadena, and from Timothy Whorf and Warren White of the Scripps Institute of Oceanography.

REFERENCES

Abawi GY, Dutta SC, McClymont D, Treloar NC, Ritchie J, Harris TR. 2001. A decision support tool for managing the impact of climate variability on water resources. In *Modelling and Simulation Society of Australia and New Zealand Conference*, Australian National University, Canberra, Australia, 10–13 December.

Brosche P, Seiler U, Sundermann J, Wunsch J. 1989. Periodic changes in Earth's rotation due to oceanic tides. *Astronomy and Astrophysics* **220**: 318–320.

Burroughs WJ. 1992. *Weather Cycles: Real or Imaginary?* Cambridge University Press: Cambridge.

Cartwright DE, Tayler RJ. 1971. New computations of the tide-generating potential. *Geophysical Journal of the Royal Astronomical Society* **23**: 45–74.

Cartwright DE. 1974. Years of peak astronomical tides. *Nature* **248**: 656–657.

Cerveny RS, Shaffer JA. 2001. The moon and El Nino. *Geophysical Research Letters* **28**: 25–28.

Chao BF, Ray RD. 1997. Oceanic tidal angular momentum and Earth's rotation variations. *Progress in Oceanography* **40**: 399–421.

Currie RG. 1987. Examples and implications of 18.6- and 11-year terms in world weather records. In *Climate: History, Periodicity and Predictability*, Rampino MR, Newman WS, Sanders JE, Konigsson LK (eds). Van Nostrand Reinhold: New York; 379–403.

Currie RG, Vines RG. 1996. Evidence for luni-solar M_n and solar cycle S_c signals in Australian rainfall data. *International Journal of Climatology* **16**: 1243–1265.

De Rop W. 1971. A tidal period of 1800 years. *Tellus* **23**: 261–262.

Dickey JO. 1993. Atmospheric excitation of the Earth's rotation: progress and prospects via space geodesy. In *Contributions of Space Geodesy to Geodynamics: Earth Dynamics*. Geodynamics Series, vol. 24. American Geophysical Union: Washington, DC; 55–70.

Doodson AT. 1921. The harmonic development of the tide-generating potential. *Proceedings of the Royal Society of London, Series A* **100**: 305–329.

Eubanks TM, Steppe JA, Dickey JD, Callahan PS. 1985. A spectral analysis of the Earth's angular momentum budget. *Journal of Geophysical Research* **90**: 5385–5404.

Eubanks TM. 1993. Variations in the orientation of the Earth. In *Contributions of Space Geodesy to Geodynamics: Earth Dynamics*. Geodynamics Series, vol. 24. American Geophysical Union: Washington, DC; 1–54.

Fairbridge RW, Sanders JE. 1987. The sun's orbit, A.D. 750–2050: basis for new perspectives on planetary dynamics and Earth–Moon linkage. In *Climate: History, Periodicity and Predictability*, Rampino MR, Sanders JE, Newman WS, Konigsson LK (eds). Van Nostrand Reinhold: New York.

Folland CK, Parker DE, Colman AW, Washington R. 1999. Large scale modes of ocean surface temperature since the late nineteenth century. In *Beyond El Nino: Decadal and Interdecadal Climate Variability*, Navarra A (ed.). Springer: New York; 73–102.

Gershunov A, Barnett TP. 1998. Interdecadal modulation of ENSO teleconnections. *Bulletin of the American Meteorological Society* **79**: 2715–2725.

Hammer GL, Holzworth DP, Stone RC. 1996. The value of skill in seasonal climate forecasting to wheat crop management in a region with high climatic variability. *Australian Journal of Agricultural Research* **47**: 717–737.

Hibler WD III, Johnsen SJ. 1979. The 20-year cycle in Greenland ice core records. *Nature* **280**: 481–483.

Hide R, Birch NT, Morrison LV, Shea DJ, White AA. 1980. Atmospheric angular momentum fluctuations and changes in the length of the day. *Nature* **286**: 114–117.

Keeling CD, Whorf TP. 1997. Possible forcing of global temperatures by the oceanic tides. *Proceedings of the National Academy of Sciences of the United States of America* **94**: 8321–8328.

Keeling CD, Whorf TP. 2000. The 1800-year oceanic tidal cycle: a possible cause of rapid climate change. *Proceedings of the National Academy of Sciences of the United States of American* **97**: 3814–3819.
Lamb HH. 1972. *Climate: Present, Past and Future*. Methuen: London.
Lambeck K. 1980. *The Earth's Variable Rotation: Geophysical Causes and Consequences*. Cambridge University Press: Cambridge.
Langley RB, King RW, Shapiro II, Rosen RD, Salstein DA. 1981. Atmospheric angular momentum and the length of the day: a common fluctuation with a period near 50 days. *Nature* **294**: 730–733.
Latif M. 1999. Dynamics of interdecadal variability in coupled ocean–atmosphere models. In *Beyond El Nino: Decadal and Interdecadal Climate Variability*, Navarra A (ed.). Springer: New York; 213–250.
Latif M, Barnett TP. 1996. Decadal climate variability over the North Pacific and North America: dynamics and predictability. *Journal of Climate* **9**: 2407–2422.
Madden RA, Julian PR. 1971. Detection of a 40–50 day oscillation in the zonal wind in the tropical Pacific. *Journal of the Atmospheric Sciences* **28**: 702–708.
Mantua NJ, Hare SR, Zhang Y, Wallace JM, Francis RC. 1997. A Pacific interdecadal climate oscillation with impacts on salmon production. *Bulletin of the American Meteorological Society* **78**: 1069–1079.
Meeus J. 1991. *Astronomical Algorithms*. Willman-Bell: Richmond.
Meinke H, Power S, Allan R, Potgieter A, Stone R, deVoil P. 2000. Impact of decadal to multidecadal climate variability on Australian agriculture. In *7th National Australian Meteorological and Oceanographic Society Conference*, AMOS Conference (eds). AMOS Publication no. 16. AMOS: Melbourne; 85.
Munk WH, MacDonald GJF. 1960. *The Rotation of the Earth: a Geophysical Discussion*. Cambridge University Press: Cambridge.
Munk WH, Wunsch C. 1998. Abyssal recipes II: energetics of tidal and wind mixing. *Deep Sea Research I* **45**: 1977–2010.
Mysak LA. 1999. Interdecadal variability at northern high latitudes. In *Beyond El Nino: Decadal and Interdecadal Climate Variability*, Navarra A (ed.). Springer: New York; 1–24.
Navarra A (ed.). 1999. *Beyond El Nino: Decadal and Interdecadal Climate Variability*. Springer: New York.
Neelin JD, Battisti DS, Hirst AC, Jin F-F, Wakata Y, Yamagata T, Zebiak SE. 1998. ENSO theory. *Journal of Geophysical Research* **103**: 14 261–14 290.
O'Brien DP, Currie RG. 1993. Observations of the 18.6-year cycle in air pressure and a theoretical model to explain certain aspects of this signal. *Climate Dynamics* **8**: 287–298.
Power S, Casey T, Folland C, Colman A, Mehta V. 1999. Inter-decadal modulation of the impact of ENSO on Australia. *Climate Dynamics* **15**: 319–324.
Schopf PS, Suarez MJ. 1988. Vacillations in a coupled ocean–atmosphere model. *Journal of the Atmospheric Sciences* **45**: 549–566.
Shaffer JA, Cerveny RS. 1998. Long-term equilibrium tides. *Journal of Geophysical Research* **103**: 18 801–18 807.
Stone RC, Auliciems A. 1992. SOI phase relationships with rainfall in eastern Australia. *International Journal of Climatology* **12**: 625–636.
Stone RC, Hammer GL, Marcussen T. 1996. Prediction of global rainfall probabilities using phases of the southern oscillation index. *Nature* **384**: 252–255.
Tsien HS. 1954. *Engineering Cybernetics*. McGraw-Hill: New York.
Wood FJ. 1986. *Tidal Dynamics: Coastal Flooding, and Cycles of Gravitational Force*. D. Reidel: Norwell, MA; pp. 558.
Yoder CF, Williams JG, Parke ME. 1981. Tidal variations of Earth rotation. *Journal of Geophysical Research* **86**: 881–891.
Zhang Y, Wallace JM, Battisti DS. 1997. ENSO-like interdecadal variability: 1900–93. *Journal of Climate* **10**: 1004–1020.

